Kashf Journal of Multidisciplinary Research
Vol: 02 - Issue 05 (2025)
P-ISSN: 3007-1992 E-ISSN: 3007-200X
https://kjmr.com.pk

SYNTHESIS AND INVESTIGATION OF ELECTROCHEMICAL PROPERTIES OF REDUCED GRAPHENE OXIDE-BASED COMPOSITES

Qadeer Ahmed [*1], Waqas Jahangir [2], Hina Tahir [3], Ansar Abbas [4], Shahid Ali [5], Muhammad Arif [6], Eraj Muzaffar [7], Jigar Allah Ditta [*8]

[1,2,7,8] Department of Chemistry, Lahore Garrison University (LGU) Sector-C Avenue-4, Phase 6 DHA, Lahore, Pakistan.
[3] National Agricultural Research Centre, Islamabad, Pakistan.
[4,5] Department of Basic and Applied Chemistry, Faculty of Science and Technology, University of Central Punjab, Khayaban-e-Jinnah Road, Johar Town, Lahore-54782, Pakistan.
[6] Department of Chemistry, Minhaj University Lahore, Township Lahore, Pakistan.
***Corresponding author:** qadeerahmed941@gmail.com , jigar@lgu.edu.pk*

Article Info

Abstract

Graphene oxide-based composites enhance electrochemical performance by improving conductivity, stability, and surface area, making them ideal for energy storage, sensors, and catalytic applications. In this study, Graphene oxide-based composites were synthesized to improve their performance in different electrochemical applications. RGO-based composites were synthesized using the hydrothermal method. XRD, FTIR, and SEM Electrochemical measurements (CV) were used to characterize the synthesized material. Electrochemical measurements (CV) were observed utilizing a three-electrode setup using composite-coated Ni foam. The nature of surface-active sites was detected from the voltammograms. Among the RGO-based composites studied, RGO- MoO2 demonstrated superior capacitive performance, achieving a maximum capacitance of 1851.60 F/g at a scan rate of 10 mV/s. This outperforms both RGO-CdO (1643.70 F/g) and RGO-CuO (1206.90 F/g). The enhanced capacitance of RGO- MoO2 is attributed to its larger surface area and more porous structure, which facilitate better electrolyte accessibility and ion diffusion within the material.

Keywords:

Composite, Electrochemical, Synthesis, Voltammograms, Diffusion.

Introduction

A layer of carbon of just one atom in a honeycomb chain has been one of the most amazing material discoveries of the 21st century [1]. It can be transformed to RGO that shows many of graphene's properties, completely retaining them, but just much easier to produce in large quantities, than graphene [2]. Scientists are currently making efforts to take full advantage of the times when RGO's composite stands out in terms of composite applications [3]. The conversion from GO to RGO is a chemical reduction that accomplishes the elimination of oxygen functional groups[4]. A crucial step is the formation of RGO. GO is synthesized via oxidation or other physical/chemical modifications through which interlayer spacing is hiked, increasing the material's hydrophilicity and solubility in water and solvents[5]. The transition of GO to RGO depicts not only the way toward the most attractive features of pristine graphene [6]. A composite is joining the high electrical conductivity of one material with a high electrochemical capacity [7]. The most concise and powerful feature of composite materials used for electrochemistry is their versatility [8].The use of reduced graphene oxide (RGO)-based composites brings as an example the vast field that composite [9]. The composite materials introduce a new element of engineering in the electrochemistry tools [10]. A bad conductivity of the electricity can be low and can influence the efficiency of devices for storing and conversion of energy[11]. A cross-cutting need for the creation of new kinds of materials offering better electrical conductivity, robustness, cost-effectiveness, and specific functionalities[12]. Graphene and RGO include nanostructured composites, which are at the very core of the future of materials [13]. The main function of RGO-based composites in combating the present electrochemical materials is undoubtedly complex and immensely significant [14] . RGO-based composites is that they are more stable due to graphene's robust carbon framework that does not degrade over time[15].

RGO-based composites, particularly those with reduced graphene oxide, that have been seeking new territories [16].

Materials and Methods:

The electrochemical performance of the RGO-based composites, such as capacitance, cycling stability, and rate capability, were evaluated and compared based on the synthesis methods and composite composition. The apparatus Beakers (100 mL, 250 mL, 500 mL), Measuring cylinders (10 mL, 50 mL), Pipette (5 mL), Titration flask, Spatula, China dish, Petri dish, Aluminum foil, Filter paper, Magnetic stirrer hot plate (85-2), Electronic analytical balance, Magnetic bead, Centrifuge machine (Centrifuge 80-1), Autoclave, Thermostat oven (WHL 25-A)Tripod Stand, and Funnel and chemicals Graphite Powder, Sulphuric Acid, Potassium Permanganate, Hydrazine Hydrate, Methanol, Cadmium Chloride Hydrated, Methanol, Polyvinylidene fluoride Binder and Potassium hydroxide are used for the synthesis of Reduced Graphene Oxide-Based Composites. The RGO-based composites were synthesized through a hydrothermal process (Ex situ). Process, employing metal oxide. The frame of work for the preparation of Graphene Oxide (GO) is shown in Figure 1.

Figure 1: Synthesis of Graphene Oxide (GO)

After the preparation of Graphene Oxide (GO) Synthesis of Reduced Graphene was carried out Figure 2 illustrates the whole process.

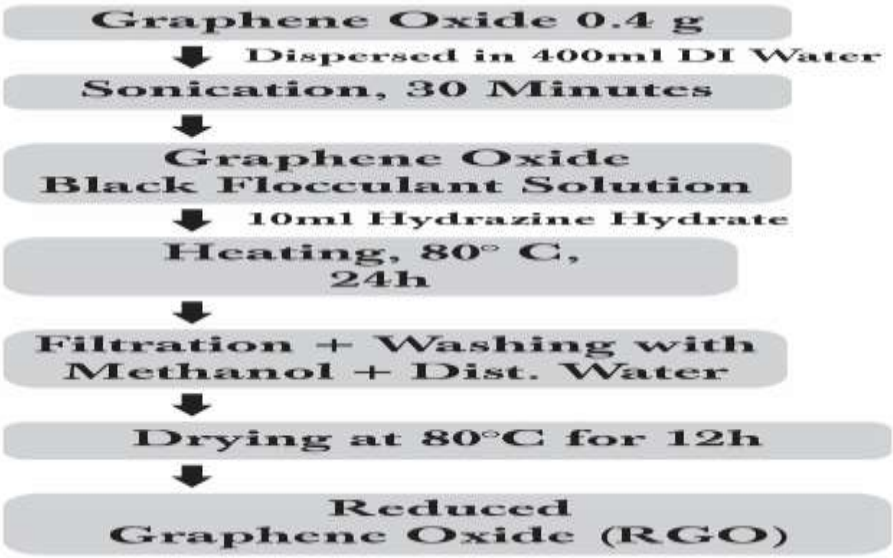

Figure 2: Synthesis of Reduced Graphene Oxide

For the synthesis of RGO composites, it is necessary to synthesize the metal oxide particles. For this purpose, a conventional hydrothermal method [41] was adopted with slight variations. In brief, salts of selected metals ($CdSO_4$, $CuSO_4$, and $MoSO_4$) were collected from Merck. Salts were used as such without further processing. 50 molar solutions of each salt were prepared in deionized water. An equal volume of salt solution and ammonium hydroxide were mixed in a beaker and sonicated for 30 minutes for homogenous mixing. After the homogenous mixing the mixture was introduced in a Teflon-lined stainless-steel autoclave, and only 70 % volume of the autoclave was filled for a smooth reaction. After

that autoclave was tightly screwed and placed in a thermostat oven at 130 ^{o}C for 24 hours for hydrothermal reaction. After 24 hours oven was switched off and allowed autoclave to cool down at room temperature. After getting residue it was washed multiple times with deionized water. After getting the washed products it was dried in the said oven at 40 ^{o}C for 12 hours after which it was collected in sample vials for further processing. The same procedure was used for each salt solution. After getting the successful. (A General Schematic presentation is given in Figure. 3)

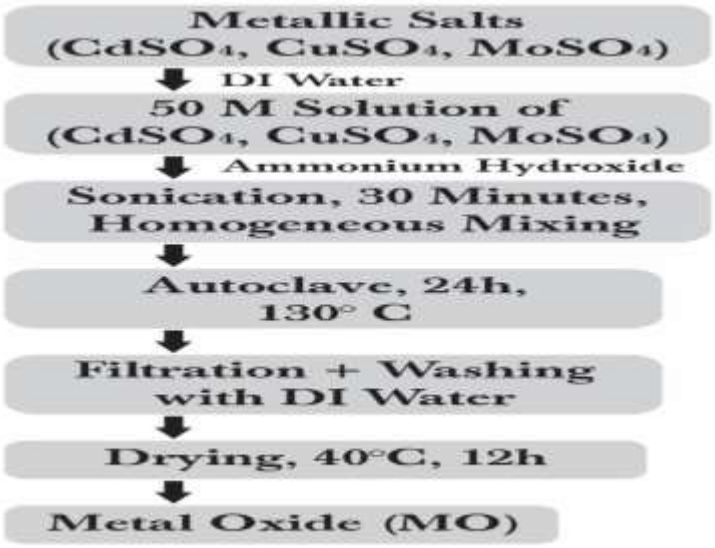

Figure 3: Synthesis of Metal Oxides (CdO, CuO, MoO_2)

A hybrid material of metal oxide and reduced graphene oxide was prepared using a hydrothermal process (Ex situ). Synthesis of metal oxide and RGO composite was initiated by mixing 0.4g metal oxide and 0.4g RGO powder in separate beakers in 20 ml DI water and then mixing both solutions and sonicated for 30 minutes. The mixture was set to magnetic stirring for 1 h to obtain a uniform dispersion of each metal oxide and RGO. The reaction mixture was then poured into Teflon-coated stainless steel and set at 130 ^{C} for 24 hours in a thermostat oven. After the autoclave was cooled down overnight to room temperature, the product was repeatedly washed using DI water. The resultant product was oven-dried at 40 ^{C} for 12 hrs. The sample was saved for analysis.

A potentiated was employed to study the electrochemical properties of a reduced graphene oxide-based composite. Composite-coated Ni foam was placed at the modified glassy carbon electrode (GCE), which acts as the working electrode. Fourier Transform Infrared (FTIR), X-ray diffraction Analysis (XRD), Scanning Electron Microscopy (SEM), and Cyclic Voltammetry (CV) were used for the characterization of synthesized materials.

Results and Discussion:

Crystallographic analysis results of the RGO-CdO composite are represented in Figure 4 revealing the presence of the various peaks specific to the CdO and RGO phases. The results of the prepared composite well matched with the reference JCPDS NO: 01–075–0592 that outlined the presence of the crystalline

cubic phase of CdO with crystal plane index C of (111), (200), (220), (311) and (222) at the 2θ values of 30.32°, 36.36°, 49.51°, 58.13°, and 65.34° respectively [44]. Furthermore, the peak obtained at the 2θ angle of 23.38° with crystal plane index C of (002) corresponds to the crystal plane of RGO [45]. However, no additional sharp peak was obtained in the studied sample's crystallography results, revealing the successful preparation of the studied composites with high purity.

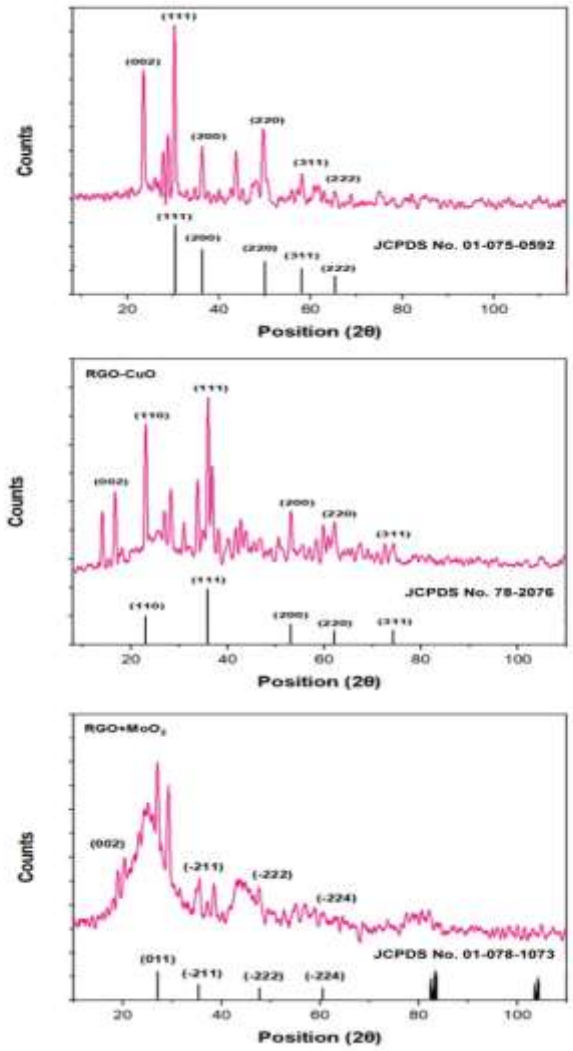

Figure 4. XRD analysis of RGO-based composites

It was observed that the results of the study well matched with the card number JCPDS No.78-2076 with crystal plane index C of (110), (111), (200), (220), and (311) that appear at the 2θ values of 23.02°, 35.96°, 53.18°, 61.99°, and 74.43° respectively corresponding to the crystalline phase of Cu as shown in Figure 5. Furthermore, the peak obtained at the 2θ angle of 23.38° with crystal plane index C of (002) corresponds to the crystal plane of RGO.

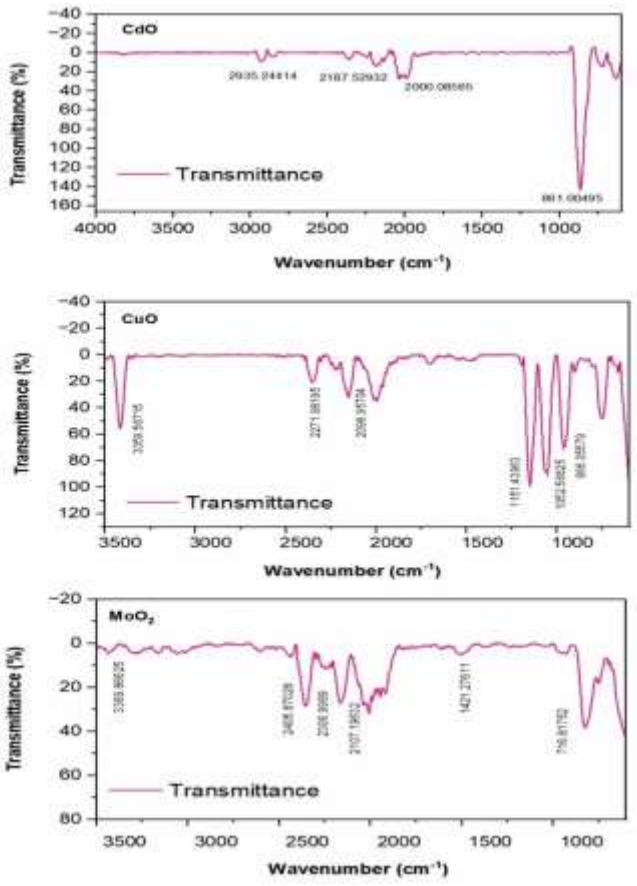

Figure 5 FTIR analysis of RGO-based composites

FTIR analysis of the prepared RGO-CdO, RGO-CuO, and RGO-MoO_2 composite was carried out within the range 4000-800 cm^{-1} and the results of the study are elaborated in Figure (4.2 a, b, and c) respectively. The FTIR study revealed the presence of various organic and inorganic functionalities, with a major proportion of anionic functional groups including oxygen-containing functional groups. In FTIR spectra when CO_2 from the atmosphere gets adsorbed onto the sample or is present in the measurement environment[61-63]. Furthermore, the peak value obtained nearly at 716.81 cm^{-1} represents the presence of Mo-O vibrations. FTIR functionalities present in each composite are shown in Table 1.

Table 1. FTIR functionalities present in each composite

Composite	Functional group	Observed values	Theoretical values
CdO	C-H stretching	2935.24 cm^{-1}	2850-3050 cm^{-1}
	Cd-O bond vibrations	861.00 cm^{-1}	800 -1000 cm^{-1}
	Cu-O bond vibrations	966.05 cm^{-1}	950-1040 cm^{-1}

CuO	O-H stretching	3359.56 cm^{-1}	3300-3600 cm^{-1}
	C-O stretching vibrations	1052.56 cm^{-1} and 1151.43 cm^{-1}	1000-1300 cm^{-1}
MoO_2	O-H stretching	3359.86 cm^{-1}	3600-3700 cm^{-1}
	Mo-O vibrations	716.81 cm^{-1}	800-1000 cm^{-1}
	CO stretching	2107.19 cm^{-1},	1900-2200 cm^{-1}

Textural properties of the prepared samples RGO-CdO, RGO-CuO and RGO-MoO_2 were investigated by scanning electron microscopy (SEM). The results of each sample at different magnifications have been summarized in Figures 6, 7 and 8. For RGO-CdO samples, results are shown in Figure 6 revealing the textural properties of RGO-CdO composite.

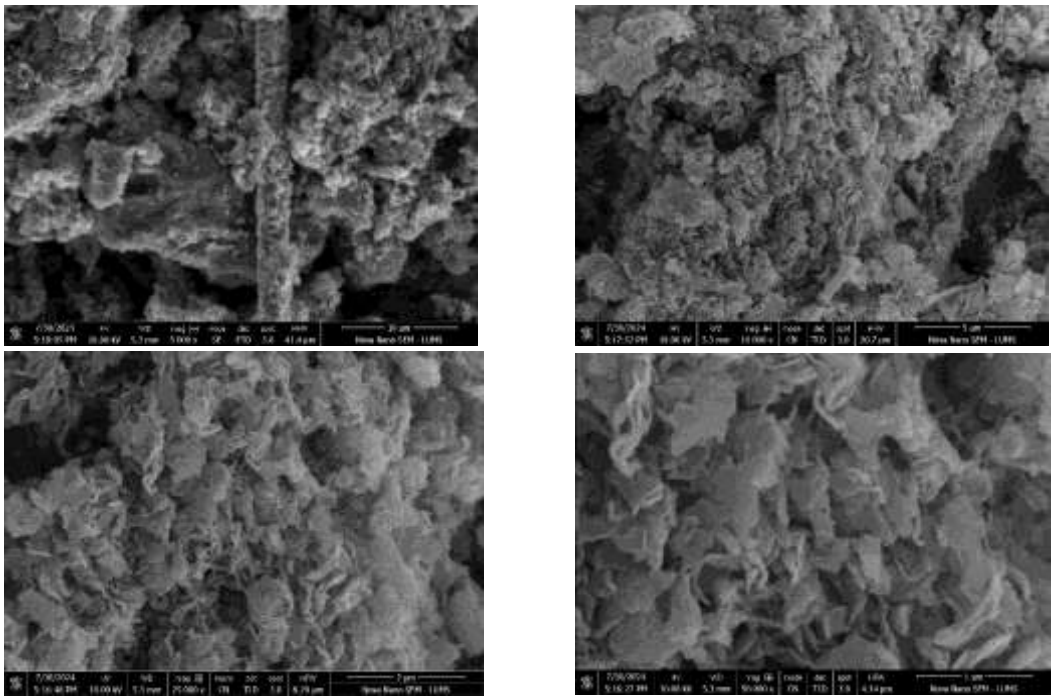

Figure 6. SEM results of RGO-CdO

The morphological analysis of the prepared RGO-CuO composite has been represented in Figure 7 highlighting the integration of CuO nanoparticles with RGO sheets. The particles of the material appeared to be shaped as small size particles having variable sizes.

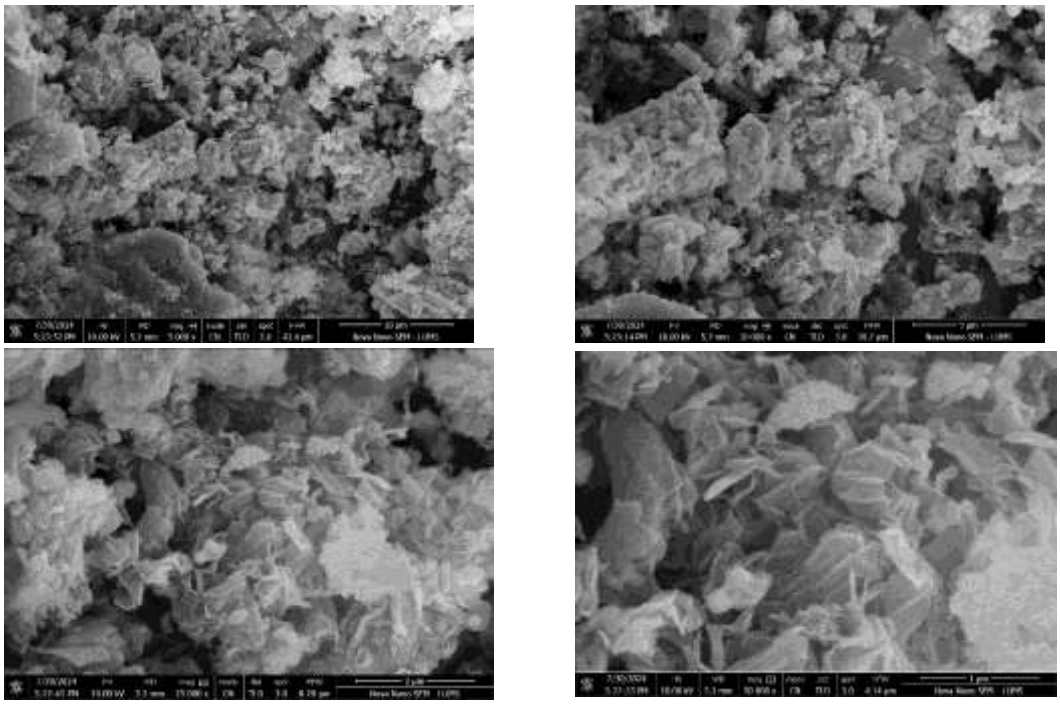

Figure 7. SEM results of RGO-CuO

The morphological analysis of the prepared RGO-MoO_2 composite is represented in Figure 8. The particles of the composites were of crystal shape having variable sizes and shapes that were widely spread over the surface of the composite. .

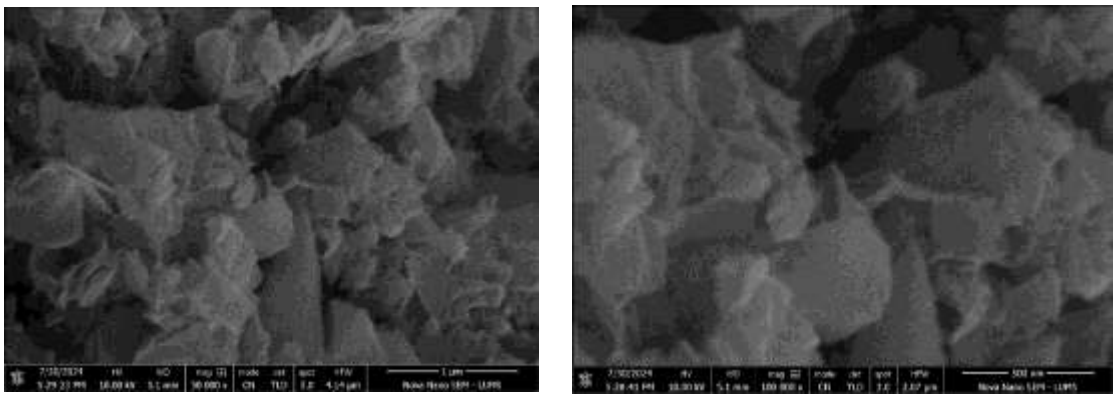

Figure 8. SEM results of RGO-MoO_2

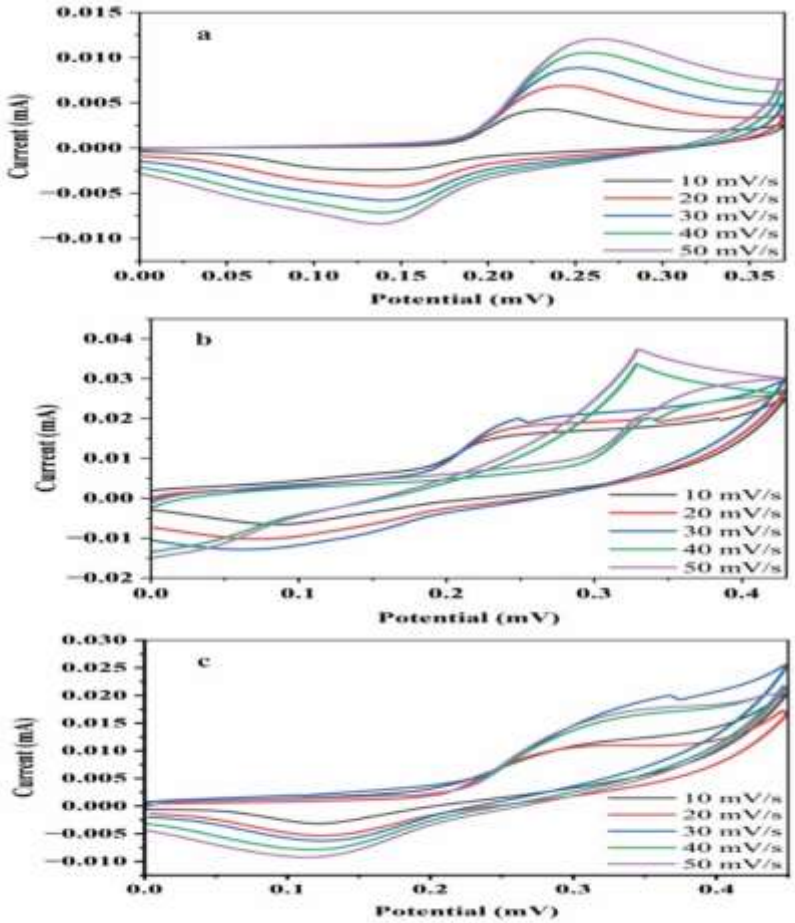

Figure 9: CV analysis of RGO-based composites

The cyclic voltammetry (CV) experiments were carried out at scan rates of 10, 20, 30, 40, and 50mVs $^{-1}$ in the range of 0.05 V to 0.5 V vs. Ag/AgCl as shown in (Figure 9) and data is displayed in Table 2. The observed redox potential and current at different scan rates of the RGO-CdO composite have been given in Table 4.1. Redox potential and current values for CV of RGO-CdO composite were 0.3911, 0.3876, 0.3926, 0.3921, and 0.3891V and 0.002, 0.0026, 0.003, 0.0033, and 0.0035A at scan rates of 10, 20, 30, 40, and 50mV/s.

Table 2. Calculation of redox current and redox potential of RGO-CdO

Scan rate (mV/s)	Anodic potential (Va) (V)	Cathodic potential (Vc) (V)	Total Redox potential (V)	Anodic current (Ia) (A)	Cathodic current (Ic) (A)	Total Redox current (A)
10	0.1587	0.2324	0.3911	-0.0022	0.0042	0.002
20	0.1417	0.2459	0.3876	-0.0042	0.0068	0.0026

30	0.1482	0.2444	0.3926	-0.0057	0.0087	0.003
40	0.1412	0.2509	0.3921	-0.0071	0.0104	0.0033
50	0.1357	0.2534	0.3891	-0.0083	0.0118	0.0035

The observed redox potential and current at different scan rates of RGO-CuO composite have been given in table 3Redox potential and current values for CV of RGO-CuO composite were 0.5629, 0.5319, 0.5329, 0.5314, and 0.5434V and 0.0185, 0.0179, 0.0192, 0.0308, and 0.0353A at scan rates of 10, 20, 30, 40, and 50mV/s. The CV curve of RGO-CuO composite clearly showed the redox peak and led to a redox reaction.

Table 3. Calculation of redox current and redox potential of RGO-CuO

Scan rate (mV/s)	**Anodic potential (Va) (V)**	**Cathodic potential (Vc) (V)**	**Total Redox potential (V)**	**Anodic current (Ia) (A)**	**Cathodic current (Ic) (A)**	**Total Redox current (A)**
10	0.2622	0.3007	0.5629	0.0014	0.0171	0.0185
20	0.2302	0.3017	0.5319	-0.0012	0.0191	0.0179
30	0.2217	0.3112	0.5329	-0.0023	0.0215	0.0192
40	0.2203	0.3111	0.5314	0.0053	0.0255	0.0308
50	0.2333	0.3101	0.5434	0.0072	0.0281	0.0353

The observed redox potential and current at different scan rates of RGO-MoO_2 composite have been given in table 4.3. Redox potential and current values for CV of RGO-MoO_2 composite were 0.574, 0.486, 0.467, 0.458, and 0.466V and 7.73, 0.0059, 0.012, 0.009, and 0.008A at scan rates of 10, 20, 30, 40, and 50mV/s. **Table 4** Calculation of redox current and redox potential of RGO-MoO_2

Scan rate (mV/s)	**Anodic potential (Va) (V)**	**Cathodic potential (Vc) (V)**	**Total Redox potential (V)**	**Anodic current (Ia) (A)**	**Cathodic current (Ic) (A)**	**Total Redox current (A)**
10	0.226	0.348	0.574	7.718	0.012	7.73
20	0.137	0.349	0.486	-0.005	0.0109	0.0059
30	0.124	0.343	0.467	-0.006	0.018	0.012
40	0.116	0.342	0.458	-0.007	0.016	0.009
50	0.123	0.343	0.466	-0.009	0.017	0.008

Capacitance of RGO-CdO composite at different scan rate have been given in table5.

Table 5. The capacitance of RGO-CdO composite

SR(mV/s)	2*SR*m*v	Area	Area*1000	Cs (F/g) A/[2mk($V_1 - V_2$)]
10	0.12	0.19724	197.24	1643.73
20	0.24	0.25917	259.17	1079.89
30	0.36	0.32450	324.50	901.40
40	0.48	0.42343	423.43	882.14
50	0.6	0.50140	501.40	835.68

Among the scan rates tested, the RGO-CdO composite exhibited its highest capacitance at 10 mV/s, reaching a value of 1643.73 F/g.

Table 6. The capacitance of RGO-CuO composite

SR(mV/s)	2*SR*m*v	Area	Area*1000	Cs (F/g) A/[2mk($V_1 - V_2$)]
10	0.12	0.14482	144.82	1206.90
20	0.24	0.21825	218.25	909.40
30	0.36	0.28208	282.08	783.57
40	0.48	0.29429	294.29	613.11
50	0.6	0.31936	319.36	532.27

Table 7. The capacitance of RGO-MoO_2 composite at different

SR(mV/s)	2*SR*m*v	Area	Area*1000	Cs (F/g) A/[2mk($V_1 - V_2$)]
10	0.08	0.14812	148.12	1851.60
20	0.16	0.20571	205.71	1285.74
30	0.24	0.26387	263.87	1099.47
40	0.32	0.29687	296.87	927.73
50	0.4	0.33265	332.65	831.63

Among the scan rates tested, the RGO-MoO_2 composite exhibited its highest capacitance at 10 mV/s, reaching a value of 1851.60 F/g.

Comparison between the capacitance of RGO-based composites at different scan rates has been given in table 8.

Table 8. The capacitance of RGO-MoO_2 composite at different

Materials	Scan Rate (mV/s)	Capacitance (F/g)
RGO-CdO	10	1643.70
RGO-CuO	10	1206.90
RGO-MoO_2	10	1851.60

Among the RGO-based composites studied, RGO-MoO_2 demonstrated superior capacitive performance, achieving a maximum capacitance of 1851.60 F/g at a scan rate of 10 mV/s. This outperforms both RGO-CdO (1643.70 F/g) and RGO-CuO (1206.90 F/g). The enhanced capacitance of RGO-MoO_2 is attributed to its larger surface area and more porous structure, which facilitate better electrolyte accessibility and ion diffusion within the material.

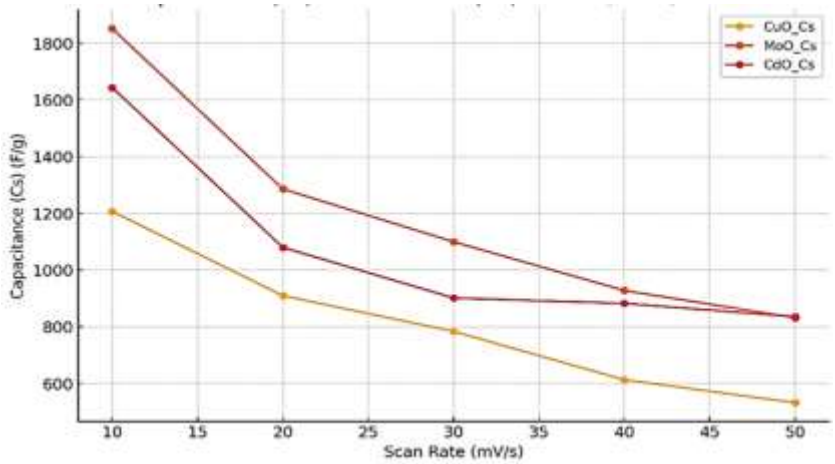

Figure 10. Capacitance vs different scan rates

A comparison of Electrochemical studies of RGO-based composites with reported work has been given in Table 10.

Table 10. A comparison of Electrochemical studies of RGO-based composites

Material	**Scan Rate (mV/s)**	**Specific Capacitance (F/g)**	**Method**	**Reported Work 1**	**Reported Work 2**
CuO	10	1206.91	Hydrothermal[69, 70]	1025	800
	20	909.41		900	750
	30	783.58		850	700
	40	613.12		800	650
	50	532.27		750	600
MoO_2	10	1851.61	Hydrothermal[1, 71]	1667	1500
	20	1285.74		1500	1300
	30	1099.47		1300	1100
	40	927.73		1224	1000
	50	831.63		1100	900

Specific capacitance was measured at different scan rates of the synthesized materials compared with the already reported material. It is observed that RGO- CuO has greater specific capacitance at 10 mV/s than

already reported. Similarly, RGO- MoO_2 has greater specific capacitance at 10mV/s than already synthesized. It can be concluded that the currently synthesized material has better specific capacitance than already reported work but only at 10 mV/s. It is further suggested that some modifications can also be made in the mythology to enhance the energy storage capacity of the material. Specific capacitance was measured at different scan rates of the synthesized materials compared with the already reported material. It is observed that RGO- CuO has greater specific capacitance at 10 mV/s than already reported. Similarly, RGO- MoO_2 has greater specific capacitance at 10mV/s than already synthesized. It can be concluded that the currently synthesized material has better specific capacitance than already reported work but only at 10 mV/s. It is further suggested that some modifications can also be made to enhance the energy storage capacity of the material.

Conclusions:

The synthesized RGO and metal oxide-based composites were characterized via XRD, SEM, LSV and CV. CV was performed on prepared electrodes at different scan rates of 1 M KOH electrolyte. The CV analysis also confirms these results of the electrode materials. The nature of surface-active sites was detected from the voltammograms. The stability of the electrode is measured after repeating the CV cycles to the given potential current response. Among the RGO-based composites studied, RGO-MoO_2 demonstrated superior capacitive performance, achieving a maximum capacitance of 1851.60 F/g at a scan rate of 10 mV/s. This outperforms both RGO-CdO (1643.70 F/g) and RGO-CuO (1206.90 F/g). The enhanced capacitance of RGO-MoO_2 is attributed to its larger surface area and more porous structure, which facilitate better electrolyte accessibility and ion diffusion within the material. The electrochemical activity of the RGO-based composites shows good stability and consistency in peak potential, while the current increases with scan rate, suggesting efficient charge transfer kinetics. The data provides insights into the electrochemical behavior of the nanoparticles, which can be useful for understanding their performance in practical applications such as sensors, batteries, or catalysis.

References

(1) Ahmed, A.; Singh, A.; Young, S.-J.; Gupta, V.; Singh, M.; Arya, S. Synthesis techniques and advances in sensing applications of reduced graphene oxide (rGO) Composites: A review. Composites Part A: Applied Science and Manufacturing 2023, 165, 107373.

(2) Yang, M.; Wang, L.; Lu, H.; Dong, Q.; Li, H.; Liu, S. Graphene and graphene-like carbon nanomaterials-based electrochemical biosensors for phytohormone detection. Carbon Letters 2023, 33 (5), 1343-1358.

(3) Ahmad, F.; Zahid, M.; Jamil, H.; Khan, M. A.; Atiq, S.; Bibi, M.; Shahbaz, K.; Adnan, M.; Danish, M.; Rasheed, F. Advances in graphene-based electrode materials for high-performance supercapacitors: A review. Journal of Energy Storage 2023, 72, 108731.

(4) Kallawar, G. A.; Bhanvase, B. A.; Sathe, B. R. Sonochemically prepared bismuth doped titanium oxide-reduced graphene oxide (Bi@ TiO2-rGO) nanocomposites for effective visible light photocatalytic degradation of malachite green. Diamond and Related Materials 2023, 139, 110423.

(5) Das, P.; Deoghare, A. B.; Maity, S. R. Enhanced Morphological, Mechanical and Dielectric Properties of Paraffin Wax Incorporated with Polyaniline (PANI) and Reduced Graphene Oxide (RGO) nanocomposites. Diamond and Related Materials 2023, 139, 110361.

(6) Mozaffarpour, F.; Hassanzadeh, N.; Vahidi, E. Synthesis, characterization and life cycle assessment of electrochemically exfoliated KOH-activated holey graphene. Frontiers of Environmental Science & Engineering 2023, 17 (12), 155.

(7) Bhujel, R.; Rai, S.; Deka, U.; Swain, B. P. Electrochemical, bonding network and electrical properties of reduced graphene oxide-Fe2O3 nanocomposite for supercapacitor electrodes applications. Journal of Alloys and Compounds 2019, 792, 250-259.

(8) Huang, C.-Y.; Lin, Y.-C.; Chung, J. H.; Chiu, H.-Y.; Yeh, N.-L.; Chang, S.-J.; Chan, C.-H.; Shih, C.-C.; Chen, G.-Y. Enhancing cementitious composites with functionalized graphene oxide-based materials: Surface chemistry and mechanisms. International Journal of Molecular Sciences 2023, 24 (13), 10461.

(9) Bansal, K.; Singh, J.; Dhaliwal, A. Synthesis of silver-decorated nanocomposite based on reduced graphene oxide and its electrochemical performance. Fullerenes, Nanotubes and Carbon Nanostructures 2023, 31 (3), 277-287.

(10) Sase, T. J.; Daring, K. E.; Bioltif, Y. E. Synthesis and Medical Application of 3D Graphene Materials. Indonesian Journal of Multidisciplinary Science 2023, 2 (5), 2521-2540.

(11) Amirzade-Iranaq, M. T.; Omidi, M.; Bakhsheshi-Rad, H. R.; Saberi, A.; Abazari, S.; Teymouri, N.; Naeimi, F.; Sergi, C.; Ismail, A. F.; Sharif, S. MWCNTs-TiO2 incorporated-Mg composites to

improve the mechanical, corrosion and biological characteristics for use in biomedical fields. Materials 2023, 16 (5), 1919.

(12) Khan, Q.; Sayed, M.; Gul, I. Titania/reduced graphene oxide nanocomposites (TiO2/rGO) as an efficient photocatalyst for the effective degradation of brilliant green in aqueous media: effect of peroxymonosulfate and operational parameters. Environmental Science and Pollution Research 2023, 30 (27), 71025-71047.

(13) Mehta, N.; Fouad, S.; Baradacs, E.; Parditka, B.; Atyia, H.; Pal, S.; Erdelyi, Z. Multilayer stack structural designing of titania and zinc white using atomic layer deposition (ALD) technique and study of thermally governed dielectric dispersion and conduction under alternating electric fields. Journal of Materials Science: Materials in Electronics 2023, 34 (8), 708.

(14) Dik, G.; Ulu, A.; Ateş, B. Synthesis and Biomedical Applications of Polymer-Functionalized Magnetic Nanoparticles. Nanofabrication 2023, 8.

(15) Zhu, Z.; Liu, Y.; Xian, G.; Wang, Y.; Wu, C.; Peng, X.; Wang, J.; Kong, L. Effect of compound coupling agent treatment on mechanical property and water absorption of hollow glass microspheres/epoxy composite. Macromolecular Research 2023, 31 (8), 771-779.

(16) Bhattacharyya, S. K.; Maiti, S.; Das, N. C.; Banerjee, S. Antibacterial and Antiviral Functional Materials Based on Polymer Nanocomposites. In Antibacterial and Antiviral Functional Materials, Volume 1, ACS Publications, 2023; pp 171-202.